Int J CARS (2010) 5 (Suppl 1):S324–S374
DOI 10.1007/s11548-010-0471-2

Gynecology brachytherapy applicator pose reconstruction in MR images

A. Lasso[1], M. Kelemen[2], T. Haidegger[2], C. Kirisits[3], G. Fichtinger[1]
[1]Queen's University, School of Computing, Kingston, Canada
[2]Budapest University of Technology and Economics, Department of Control Engineering and Information Technology, Budapest, Hungary
[3]Medical University of Vienna, Department of Radiotherapy, Vienna, Austria

Keywords Registration · MRI · Brachytherapy

Purpose

Intracavitary brachytherapy is commonly used in the treatment of cervical cancer. Accurate geometrical information of the tumour, surrounding structures, and brachytherapy applicator is required for the definition of an optimal treatment plan. Magnetic resonance (MR) imaging provides an excellent definition of the anatomical structures, but the possible source path inside the applicator is not directly visible with this image modality [1]. Hence the goal of this research is to develop an automatic algorithm for recovering the full pose (position and orientation) of a brachytherapy ring applicator in MR images, which can be directly used to digitize the source path inside the 3D MRI dataset.

Methods

The pose of the applicator is recovered by registering a 3D MR image of the applicator to the patient's MR image.

1. Synthetic MR image of the applicator

We chose the Vienna Ring applicator (Nucletron, Veenendaal, The Netherlands) for this study, but the same method can be applied to other applicators. The applicator's material typically does not respond to MR excitation and it appears as dark region (low-intensity voxels) on the images. The ring component of the applicator contains cylindrical holes for guiding interstitial needles. When the applicator is inserted into the patient, body fluids fill up the guide holes that appear as high-intensity sticks in the images.

To reproduce this appearance, we constructed a 3D geometrical model of the applicator (Fig. 1a). Then the model is turned into an MR image volume by setting voxel intensities as follows. Voxels inside the tubes of the applicator are set to a predefined dark value and voxels inside the holes are set to a predefined bright value, while all remaining voxels are set to zero (Fig. 1b). Modeling and image volume creation were implemented with the open-source Visualization Toolkit (www.vtk.org) software library.

2. Registration

We used 3D Slicer (www.slicer.org), an open-source medical image visualization and analysis software to register the synthetic applicator volume and the patient's MR volume (Fig. 2). 3D Slicer supports a number of different registration methods, from which we chose volume-to-volume registration with Mattes mutual information similarity metric, versor rigid transform, Fletcher-Reeves & Polak-Ribiere optimizer, and linear image interpolation. A mask is provided for the registration algorithm to exclude voxels of zero value from computing the metrics.

3. Test framework

A test framework was developed to generate synthetic patient MR image volumes with known ground truth for applicator position and orientation. Synthetic patient MR image volumes were created by merging real patient MR images with a synthetic volume of the applicator, in a known pose. The synthetic applicator volume had the same size and spacing as the patient image volume. The merged volume contains the applicator image voxels in those positions where the applicator voxels are not zero, and the patient image voxels in all other positions. To make the resulting image more realistic, random noise (with Rician distribution) was added to the applicator voxels.

Results

The registration algorithm was tested on 6 synthetic patient image volumes, with a random initial pose within 5 mm/degrees from the ground truth. The algorithm converged in all cases, average registration error was 0.12 mm (SD = 0.04 mm), average execution time was 27 seconds.

Preliminary testing was performed on a clinical image volume. In this case, registration error was significantly higher, about 3 mm, most probably due to differences in the appearance of the applicator on the real and the synthetic image.

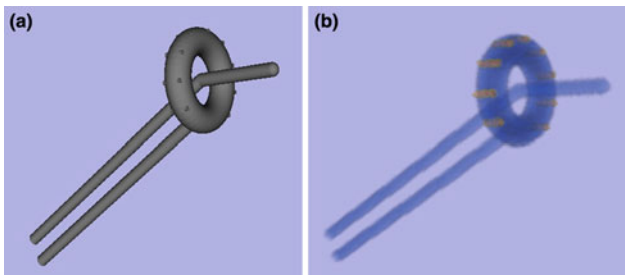

Fig. 1 **a**. Three-dimensional model of the Vienna Applicator (left), **b**. Volume rendered image of the synthetic MR volume generated from the model. Dark voxels are rendered in blue, light voxels are rendered in yellow, zero-valued voxels are transparent (right)

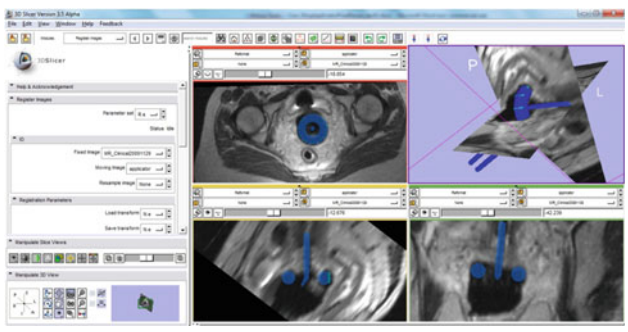

Fig. 2 Registration of the applicator image to the patient image in 3D Slicer

Conclusion
The feasibility of applicator pose reconstruction was successfully demonstrated. The registration works robustly on synthetic images with an excellent accuracy and an acceptable execution time. Initial tests indicate that our method needs further improvements to work accurately on real clinical images.

Reference

[1] Kirisits et al. The Vienna applicator for combined intracavitary and interstitial brachytherapy of cervical cancer: design, application, treatment planning, and dosimetric results, Int. J. Radiation Oncology Biol. Phys., Vol. 65, No. 2, pp. 624–630, 2006.

Comparison of respiratory monitoring system

Y. Otani[1], Y. Kumazaki[1], H. Sekine[1], E. Imabayashi[1], I. Fukuda[1], N. Tsukamoto[1], T. Teshima[2], T. Dokiya[1]

[1]Saitama Medical University International Medical Center, Dept. of Radiation Oncology, Saitama, Japan
[2]Osaka University, Medical Physics and Engineering, Osaka, Japan

Keywords Respiratory monitoring system · Respiratory gating · 4DCT

Purpose
Four-dimensional positron emission tomography/computed tomography (4DPET/CT) is widely used in the treatment planning of respiratory gated radiotherapy (RGRT) to evaluate tumor motion. In RGRT, respiratory monitoring systems are used to detect the respiratory phase of patients for 4DPET/CT and linear accelerator (linac). Generally, identical respiratory monitoring systems are used for both 4DPET/CT and linac. However, different respiratory monitoring systems are used for 4DPET/CT and linac because none of the currently available system can be connected to both the 4DPET/CT (Biograph, Siemens Medical Solutions, IL) and linac (Trilogy, Varian Medical systems, Palo Alto, CA). Thus, 4DPET/CT images cannot be used for treatment planning. The purpose of this study is to evaluate the correlation between the signals generated by different respiratory monitoring systems.

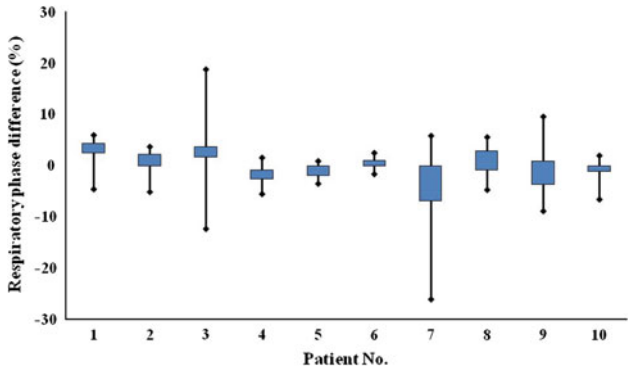

Fig. 1 Box plot of the differences between respiratory phases determined by the RPM and AZ-733V systems. The 50% interquartile range, range are displayed. A positive value indicates that the tag $_{(RPM)}$ is sent before the tag $_{(AZ\text{-}733V)}$

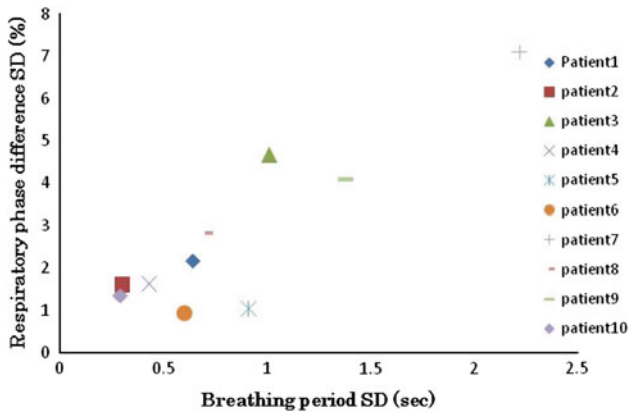

Fig. 2 Respiratory phase difference SD vs. respiratory period SD for all patients

Methods
We recruited ten patients (male, 7; female, 3) with a median age of 75 years (range, 57-84 years). We used two respiratory monitoring systems, Real-time Position Management (RPM) system (ver. 1.6.5, Varian Medical systems, Palo Alto, CA) and AZ-733V system (ver. 3.0A, Anzai MEDICAL, Shinagawa, Tokyo). To fix that patient position during data acquisition, the patients were immobilized using a body fix device (EBS-2000, Engineering System, Matsumoto, Nagano), and their arms were raised using body shell (ESFORM, Engineering System, Matsumoto, Nagano). A part of the body shell in the abdominal region was cut out and removed, and both the respiratory monitoring systems were positioned in this region. A marker block was placed on the abdomen, at a point between the xiphoid process and umbilicus, and a pressure sensor was inserted between the body shell and the abdomen, near the marker block. Using the signals from both the respiratory monitoring systems, we analyzed the relationship between the amplitude peak and tag for each patient. The phase difference was calculated from the time shift of the tag. The definitions of all amplitude peak and tag generated were as follows.

- peak $_{(RPM)}$: point of amplitude peak from respiratory signal of the RPM system.
- peak $_{(AZ\text{-}733V)}$: point o f amplitude peak from respiratory signal of the AZ-733V system.
- tag $_{(RPM)}$: point of end-inspiration by the RPM system is determined by algorithm.
- tag $_{(AZ\text{-}733V)}$: point of end-inspiration by the AZ-733V system is determined by algorithm.

Results
The correlation factor between RPM and AZ-733V signals for patients varies from 0.940 to 0.994, with a median of 0.990. The differences between the respiratory phases determined by the RPM and AZ-733V systems are shown in Fig. 1. A positive value indicates that the tag $_{(RPM)}$ is sent before the tag $_{(AZ\text{-}733V)}$. The value of median $\pm$ standard deviation (SD) for the phase difference data obtained for the patients varied from -4.3 $\pm$ 7.1% to 3.5 $\pm$ 2.2%. A comparison of SDs of the respiratory phase difference data and those of the breathing period data for all the patients gave a correlation factor of 0.887 (Fig. 2). However, the correlation factor between the SDs of the respiratory phase difference data and those of the abdominal displacement data was 0.584.

Conclusions
We evaluated the respiratory signal and tag for two respiratory monitoring systems. The peak $_{(RPM)}$ corresponds well to those of peak $_{(AZ\text{-}733V)}$. But, the points of tag $_{(RPM)}$ and tag $_{(AZ\text{-}733V)}$ were different in the some respiratory patterns, which lead to a phase difference. An increase in the SD of the breathing period data tends to cause an increase in the SD of the respiratory phase difference. Taken together, our findings indicate that the accuracy of amplitude-based gating achieved by the use of the combination use of the RPM and AZ-733V systems is identical to that achieved by using the same respiratory monitoring system with the 4DPET/CT and the linac. Ensuring the regularity of the breathing period effectively minimizes the phase difference between the two systems.